

# Phase Shift MRI in Assessment of Vertebral Compression Fracture: Trial for a New Scoring System

**Khaled Matrawy**

Alexandria University

**Nadia Abdel Fattah**

Alexandria University

**Abdel Aziz ElNekidy**

Alexandria University

**Mohamed Abdel Gawad**

Menofeya university, Egypt

**Alaa Elnaggar**

Alexandria University

**Gihan Shehata**

Alexandria University

**Ihab Reda**

Alexandria University

**Adel Shalabi** (✉ [adel.shalabi@akademiska.se](mailto:adel.shalabi@akademiska.se))

Uppsala University

---

## Research Article

**Keywords:** Chemical shift, MRI, Vertebral compression fracture, New Scoring system

**Posted Date:** December 28th, 2020

**DOI:** <https://doi.org/10.21203/rs.3.rs-129229/v1>

**License:**   This work is licensed under a Creative Commons Attribution 4.0 International License.

[Read Full License](#)

---

# Abstract

## Purpose

To assess the value of in /opposed-phase quantitative chemical shift MRI in differentiating malignant from benign vertebral compression fractures (VCF).

## Patients and methods

Twenty patients (8 men), mean age 56 years, with low back and radiological proof of VCF were included in the study. MRI of spine with standard conventional sequences and special chemical shift sequence (in/opposed phase) as well as diffusion weighted imaging were performed (at 1.5 Tesla). Quantitative image analysis of regions of interest (ROI) on the abnormal marrow in the compressed (study group) and related normal vertebra in same patient (control group) was done in each patient. The signal intensity ratio (SIR) of the marrow was determined by dividing the mean signal intensity on the opposed-phase and in-phase images was performed.

## Results

Mean SIR of benign VCF [ $0.6 \pm 0.27$  (range 0.23–1.1)] was significantly lower than malignant VCF values [ $1.115 \pm 0.14$  (range 0.87–1.45)] ( $p < 0.0001$ , ROC 0.97). The optimal SIR cutoff value for separating benign and malignant VCF was found to be 0.9 with a calculated sensitivity of 91.5%, specificity of 87.5% and accuracy of 90%. We also found a cut-off value of 0.9, to be a statistically significant in differentiating benign from malignant causes of VCF. If SIR of 0.91 as a cutoff is applied, with  $>0.91$  indicating malignant result and  $<0.91$  defined as a benign result.

## Conclusion

Quantitative chemical shift MR imaging could be a valuable addition to standard MR imaging techniques in differentiating benign from malignant vertebral compression fracture. We designed a new scoring system based on conventional MRI, in/opposed phase chemical shift and diffusion weighted imaging. The new scoring system may be a useful tool and add value in the diagnosis of compression vertebral fractures.

# Introduction

Spine compression fractures are a typical clinical issue, especially in elderly patients. Osteoporosis is the most widely recognized reason of compression fractures in this age group. The spine is a typical site for metastasis and composes up to 39% of all bone metastases, with resultant vertebral pathological compression fracture. At the same time compression fractures due osteoporosis seen in the same age group making it is difficult to differentiate it from osseous deposits and to choose the suitable treatment strategy (1).

Vertebral compression fractures (VCF) have imperative wellbeing ramifications for old, including incapacity and expanded mortality (1). Prevention of such fractures by suitable drugs and treatment of these high-chance patients is justified. Henceforth the early and exact determination of vertebral compression is an imperative factor in improving the clinical outcome of patients particularly with osteoporosis (2).

VCF might be characterized radiographically or as a clinical occasion. The commonness of these fractures in females aged 50 and over has been evaluated at 26% when defined as a reduction in vertebral height >15%. Retrospective assessment of case records has shown a clinical detection rate of VCF in white females of 153/100 000 person years. Of these clinically detected VCFs, 84% were associated with agony (3).

Imaging is fundamental to affirm the precise area of the damage, to survey the steadiness of the spine, and to characterize the repercussion of the injury on the spinal canal and neural foramina, just as on the spinal cord and nerve roots (4).

Traumatic spine fractures predominantly affect young men while osteoporotic fractures more in elderly women (4).

Much increasingly critical is to survey the disfigurement of the spinal trench and neural foramina. The spinal canal is often narrowed from translation and intrusion of vertebral body fragments. On sagittal views, which can be obtained through multiplanar reformation of volumetric CT data sets or from sagittal MRT images, the anterior–posterior canal diameter can be measured. Some authors have suggested measuring the cross-sectional area compromise, especially in thoracic and lumbar spine injuries (5).

The aim of this study was to assess the value of in-phase/opposed-phase quantitative chemical shift magnetic resonance imaging in differentiating malignant from benign vertebral compression fractures with the use of a new scoring system based on radiological features.

## Patients And Methods

Twenty patients including 8 men and 12 women were included in this study. Their ages ranging from 5 to 82 years; with mean age about 56 years.

The inclusion criteria included back pain and/or a neurological deficit, with or without history of minimal trauma were enrolled in this prospective study. While the exclusion criteria were patients with diffuse marrow infiltration, because we needed a normal appearing vertebral marrow to be used as internal reference control group in each patient.

Thirteen out of the twenty patients had known primary malignancy; breast cancer in eight patients, prostate cancer in two patients, ovarian cancer in one patient, hepatocellular carcinoma in one patient and metastasis from unknown origin in two patients. The remaining seven patients had no history of previous malignancy (table 1, fig 1).

All patients were followed for 18 months after the completion of the study and the final clinical diagnosis was used as the “gold standard” to classify the vertebral lesions as benign or malignant.

Ethics approval is at: Ethics committee of Faculty of Medicine- Alexandria University (IRB NO: 00012098, FWA NO: 00018699)

## **MRI imaging**

MRI examinations were performed using a standard body coil on a 1.5 Tesla super conducting MR System (Magnetom Avanto; Siemens, Erlangen, Germany).

The imaging sequences included sagittal and axial T1WI spin echo sequences with echo time (TE) 11ms, repetition time (TR) 590 ms, field of view (FOV) 300×300 mm, acquisition matrix 384×288, slice thickness 4 mm and interslice gap 4.4 mm.

Sagittal and axial T2WI with TE 91 ms, TR 3500 ms, FOV 300×300 mm, acquisition matrix 384× 269, slice thickness 4 mm and interslice gap 4.4 mm.

Patients with a history of malignancy received gadolinium as part of the routine protocol if this was believed to be necessary at the time of examination. Patients with a history of trauma did not received gadolinium.

Dual chemical shift sequences for OP and IP images with breath-holding were obtained at TR/TE 110/2.3 msec (OP images) and TR/TE 110/ 4.7 msec (IP images) respectively. The flip angle was 90°. The duration of these sequences was 32 seconds, yielding seven slices.

The imaging sequence for DWI was a multi-section, fat suppression spin-echo-type single-shot echo-planar imaging (EPI) sequence done in the sagittal plane.

All images were then sent to a PACS workstation, and areas that were of abnormal signal intensity on the T1 and T2 sequences were identified on the in-phase/opposed-phase sequences. An elliptical region of interest cursor was placed over the abnormal area on the in-phase as well as on the opposed-phase images. Three measurements of the signal intensity were made, and the average recorded. A computation of the signal intensity ratio (SIR) of the marrow on the opposed phase to signal intensity measured on the in-phase images was made.

## **Scoring system**

We assumed a scoring system made of these three imaging modalities to help in directing the assessment of collapsed vertebrae, with considering each positive finding of malignancy as a point: Conventional MRI consider convex posterior border, epidural soft tissue component in association to altered marrow signal intensity as a point. Measured SIR of the collapsed vertebra > 0.9, is considered a point. Restricted diffusion, ADC values 1 or less, is also considered a point.

The measured score of 3 points, is highly indicating malignant compression. While, the measured score of the vertebra of 2 points, is probably malignant. further confirmation is recommended. Similarly, the score of the vertebra of 0 or 1 point is highly indicating benign collapse.

## Statistical analysis

The signal intensity ratio (SIR) from the out phase – in phase sequences of the collapsed vertebrae were statistically analyzed by using SPSS version 20. A receiver operating characteristic ROC and chi-square tests were used to identify the specificity, sensitivity and significance of chemical shift sequence to differentiate benign from malignant vertebral collapse.

SIR of the collapsed vertebrae was statistically calculated by ROC to determine a cutoff value and to identify the specificity, sensitivity, positive predictive value (PPV) and negative predictive value (NPV) of ADC to distinguish benign from malignant vertebral collapse.

## Results

Among the twenty patients of vertebral collapses, 13 patients were diagnosed with malignant vertebral collapses and 7 patients with benign vertebral collapse, based on clinical, radiological, follow up and histopathological data. Most malignant vertebral collapses are due to cancer breast (fig 2 A-D) and cancer prostate (fig 3 A-G).

Two patients of the malignant group were accidentally discovered on routine MRI imaging for low back pain, One had typical morphological criteria of malignant collapse, showing posterior convex border, posterior neural arch affection with epidural soft tissue enhancing components, SIR > 1, was proved by histopathology to be metastatic from primary anaplastic carcinoma (fig 4 A-G). The other patient had multiple other vertebral deposits in the spine, acetabulum and was diagnosed pathologically to be secondary to primary lymphoma.

The nonmalignant patients were diagnosed by history, MRI, clinical follow up and CT. There were 7 patients, two of them had known history of malignancy and one with primary hepato cellular carcinoma (HCC) on follow up after TACE, complaining of low back pain. Conventional MRI revealed a single level vertebral collapse, with SIR >1. complementary CT was done, revealed degenerative changes, in the form of anterior wedging, fractured end plate, with intra vertebral disc vacuum, suggesting avascular osteonecrosis of the vertebra (Kummel's disease) (fig 5 A-G). Other patient with sizable pelvic mass, diagnosed as primary ovarian malignancy, was followed up clinically and MRI, findings revealed SIR in IP/OP similar to that of benign collapse, this patient underwent histopathological confirmation by bone biopsy from the affected vertebrae, which was negative for malignant cells, suggesting the cause of fracture was secondary to osteoporosis.

Multiple associated radiological findings were encountered incidentally among our patients with vertebral collapses shown in (fig 6, table 2).

The measured SIR (OP/IP) of the collapsed vertebrae in the out and in phase sequences are listed in table 3. It demonstrated that the SIR of the vertebral collapse due to malignant causes revealed high values, while the SIR of the benign collapses gives low values like those measured on normal vertebra.

The diffusion in the collapsed vertebrae is listed in table 4, using  $ADC = 10^{-3} \times 0.1 \text{ mm}^2/\text{sec}$  as cut off value. It demonstrated that the vertebral collapse due to malignant causes revealed restricted diffusion in twelve out of thirteen cases, with no appreciable restriction in the collapsed vertebrae in the case of Langerhans histiocytosis, while the benign collapses reveals no restriction in six out of seven cases, with definite restriction seen in the case of Kummel's disease.

### **Applying scoring system:**

The results of different imaging modalities including conventional, chemical shift as well as diffusion sequences used collectively in assessment of the collapsed vertebrae is listed in Table 5.

In the thirteen patients with malignant vertebral collapses, six of them showed the score of 3, six with score of 2 and one with score of 1 (Langerhans Histiocytosis).

In the seven patients with benign vertebral collapses, six of them showed the score of 0, while only one patient with Kummel's disease, showed a score of 2.

### **Analysis of data:**

#### **Control vertebrae**

All normal vertebrae on conventional MR images, exhibited a significant dropout in the signal intensity on out-of phase images compared with in-phase images. The mean signal intensity ratio for normal bone marrow was  $0.51 \pm 0.14$  (range 0.12–0.7).

#### **Benign vs malignant vertebral compression**

The signal intensity at T1 and T2 WI for benign and malignant compression fractures were demonstrated in table 6.

As regards the chemical shift images 18 of the 19 benign compressed vertebrae showed a signal dropout on out-phase when compared to in-phase images. One case with Kummel's disease in a known patient with history of HCC, showed no significant signal drop in out phase sequence, with  $SIR > 1$ . Complementary CT with serial follows up were done.

The mean signal intensity ratios for the benign compression fracture group and the normal marrow control group were significantly lower than SIR values for the malignant group ( $0.56 \pm 0.27$  (range 0.23–1.1) and  $1.09 \pm 0.20$  (range 0.901–1.45) respectively.  $p < .0001$  and  $p < .0001$ , respectively) (table 7).

No significant difference was found between the mean signal intensity ratios for the benign compression fracture group, and the normal marrow group ( $p = 0.61$ ), (fig 7).

Receiver operating characteristic analyses (ROC) determined the optimal SIR cutoff value to be 0.9 and area under the ROC curve, 0.97 (fig 8).

If an SIR of 0.9 as a cutoff is applied, with  $>0.9$  indicating malignant result and  $<0.9$  defined as a benign result. The new score system quantitative chemical shift in-phase/opposed-phase imaging was able to correctly detect 12 out of 13 cases of malignant vertebral compression fractures (the 13<sup>th</sup> Case of Langerhans Histiocytosis showed score of 1) and 6 out of 7 of cases of benign compression fractures (the 7<sup>th</sup> case remained border line, with score of 2, Kummel's disease) with a sensitivity of 92.31%, specificity of 85.7% and accuracy of 90% (table 8 and 9).

## Discussion

Non traumatic spine fractures are a common diagnostic problem, notably in old age patients, and always causes diagnostic dilemma (6).

In this study we assessed the value of in-phase/ opposed-phase quantitative chemical shift method, in differentiating benign from malignant vertebral fractures using a new scoring system bases on radiological data. This technique is based on unequal precession frequencies of fat and water protons, which are present in vertebral marrow (7,8).

At 1.5 T, fat and water protons are in phase with each other at a TE of 4.6 ms, and are at opposed 180 degrees with TE of 2.4 ms, because of this, the presence of roughly equal amounts of fat and water in the normal marrow, results in a suppression in the signal intensity on opposed phase images (8,9).

In osteoporosis induced fractures, although signal intensity on the conventional spin-echo sequences being abnormal, there is no abnormal marrow replacement. The presence of normal marrow fat causes a suppression in the signal intensity on opposed-phase images, while, in pathologic fractures, underlying marrow infiltration results in the lack of signal suppression on the out-of-phase images (9).

The presence of para-vertebral soft tissue masses as well as infiltration of posterior elements supports the diagnosis of malignant fracture (10).

Some morphological changes seen compression fractures may suggest benign or malignant nature, but in many cases an overlap can occur in both categories (11). Cicala et al revealed that some morphological changes plus other additional findings can suggest metastatic etiology for compression fracture such as vertebral body convex posterior border, involvement of the pedicle or posterior element, the presence of epidural or paraspinal mass and affection of other vertebral bodies by metastatic lesions (11).

Features that were described favoring osteoporotic compression fracture includes retropulsion of a posterior bone fragment, sparing of normal bone marrow signal intensity of the vertebral body, the presence of low signal intensity band on T1- and T2-weighted images, fluid signal and intra-vertebral vacuum cleft sign, as well as multiple compression fractures (11). This agrees with our study, four cases of malignant fractures were reported to have a convex posterior border as well as enhancing epidural masses, which confirmed that morphological features can assess in separating benign from malignant compression fractures.

Post contrast enhancement of compression fracture is highly suggestive of underlying malignant infiltrative process. However, Zhou et al and Dalia et al reported enhancement in 9 out of 17 of benign fractures, which all showed a signal drop on the out of phase image compared to the in phase image, a benign SIR, and were proved benign on follow up of patients, and thus the authors concluded contrast enhancement is not specific for differentiation between benign and malignant lesions (7, 12).

In our study, there were contrast enhancement in all the twelve patients of malignant fractures, which all showed no drop of signal on the out of phase image compared to the in phase image and a malignant SIR, and were proved malignant on follow up. Contrast enhanced sequences used only in patients with suspected underlying neoplastic cause. Patient with acute spine infection were excluded from our study.

So, in our study, we did not rely on contrast enhancement as a way of differentiation, but to assess the presence the epidural and para vertebral components.

The findings were expressed in the form of a ratios, by comparing the signal intensity in the abnormal bone marrow on the out-of-phase and in-phase images. This signal intensity ratio was calculated as the mean signal intensity on out-of-phase images divided by the mean signal intensity on the in-phase images.

By using this formula which was also used in studies by Eito, Ogura, Dalia and Ery, et al, we calculated a mean signal intensity ratio of  $1.72 \pm 0.14$  (range 0.8–2.96) for the neoplastic group and  $0.73 \pm 0.07$  (range 0.12–1.2) for the benign group ( $P < .0001$ ), (9, 10, 12, 13).

In our study SIR cutoff value was 0.91 to differentiate benign from malignant vertebral compression fractures, that was similar to what reported by Dalia et al (12). Our ratios was higher than that reported by Ery & Disler et al. (13,14), namely 0.8, but less than the cutoff value of 1 reported by Eito & Ogura et al, (9,10).

Our SIR cutoff value of 0.91 showed 100% sensitivity, 91.6% specificity with 95% accuracy in the separating benign and malignant vertebral compression fractures. These results agreed with Disler et al. (14) who reported 89% sensitivity and 80% specificity, as well as Ery et al. (13) who reported a 95% sensitivity and 89% specificity and Dalia et al. (12) who reported sensitivity 93%, specificity of 82%.



Geith et al. (15) had different results in which 69.2% of all osteoporotic fractures showed a hyperintense signal on opposed phase images (false-positive). No significant difference in signal intensity were found on the opposed-phase images of benign and malignant vertebral fractures and were able to reach a sensitivity of only 50%, and a specificity of 88.5%. We tried to explain their results by focusing merely on definite osteoporotic and neoplastic collapse. Cases with atypical hemangiomas showed minimal signal drop on out-of-phase images, due to the presence of microscopic quantities of fat, such cases are difficult to distinguish from malignant neoplastic on conventional routine MRI sequences.

In cases with degenerative sub-endplate sclerosis type 3, there were no appreciable signal drop on out of phase with increased SIR ratio to a suspicious level, but this is usually not problematic for diagnosis on conventional MR imaging. The term of edema like signal intensity refers to fluid hyperintense signal on T2- weighted images and is nonspecific to any pathological etiology, meaning it can result from different etiologies (e.g., degenerative, infectious, inflammatory, traumatic, and neoplastic changes). This can explain our false positive case, that was classified as malignant due to the presence of degenerative vertebral osteonecrosis in a known patient with hepatocellular carcinoma, who showed no significant signal drop in out phase images, with SIR >1, was due to sclerosis like degenerative changes, with unequal amount of fat and water. This case was confirmed by additional CT examination, which showed marked degenerative bony changes, with cortical bone defect, intra vertebral vacuum phenomenon & stability on serial follow up

False negative results were reported by Swartz et al. (16) and explained the presence of dense sclerotic or fat containing metastases. They also reported false positive pitfall, due the presence of marrow fibrosis. We didn't encounter similar cases in our cases.

The main limitations in this study were the small number of patients and unavailability of tissue diagnosis in some cases.

## Conclusion

Quantitative chemical shift MR imaging could be a valuable addition to standard MR imaging techniques in differentiating benign from malignant vertebral compression fracture. Signal intensity ratio (SIR) of 0.91 as a cutoff is applied, with >0.91 indicating malignant result and <0.91 defined as a benign. We designed a new scoring system based on conventional MRI, in/opposed phase chemical shift and diffusion weighted imaging. The new scoring system may be a useful tool and add value in the diagnosis of compression vertebral fractures.

## Declarations

Ethics approval and consent to participate: Ethics approval is at: Ethics committee of Faculty of Medicine- Alexandria University (IRB NO: 00012098, FWA NO: 00018699). Informed consent from all the participants are obtained and available Consent for publication: Not applicable Informed consent from all

the participants are obtained and available Availability of data and materials' in the manuscript: All data generated or analyzed during this study are included in this published article. All images included in the study are saved and archived by the PACS system of the radiology department- Faculty of Medicine- Alexandria University. The datasets used and analyzed during the current study available from the corresponding author on reasonable request. Competing interests: Not applicable Funding: Not applicable Authors' contributions: Khaled Matrawy idea of the work, image interpretation and wrote the main manuscript Nadia Abdel Fattah: Data collection and editing the manuscript. Abdel aziz ElNekidy: image interpretation and editing the manuscript. Mohamed Abdel Gawad: image interpretation and editing the manuscript. Alaa ElNaggar: clinical data Gihan Shehata: Biostatistics work-up Ihab Reda: idea of the work, image interpretation and editing the manuscript. Adel Shalabi: Image interpretation and Reviewing the manuscript. Acknowledgements: Not applicable Guidelines in the manuscript: All procedures were performed in accordance with relevant guidelines' in the manuscript.

## References

1. Hee SJ, Won HeeJ, kee YH. Discrimination of Metastatic from Acute Osteoporotic Compression Fractures with MR signals. *Radiographics*. 2003; 23:1 179-87
2. Esrud K, Thompson D, Cauley J, Nevitt M, Kado D, Hochberg M, Santora An, Black D Prevalent vertebral deformities predict mortality and hospitalization in older women with low bone mass. Fracture Intervention Trial Research Group. *J Am Geriatr Soc*. 2000;48:241-9
3. Kanis JA, McCloskey EV. Epidemiology of vertebral osteoporosis, *Bone*. Volume 13, Supplement 2, 2002, Pages S1-S10
4. Parizel PM, van der Zijden Æ S. Gaudino *Eur Spine J*. 2010, 19 (Suppl 1): S8–S17
5. Tsou PM, Wang J, Khoo L, Shamie AN, Holly L. A thoracic and lumbar spine injury severity classification based on neurologic function grade, spinal canal deformity, and spinal biomechanical stability. *Spine J*, 2006;6:636–647
6. Caranci F, Brunese L, Reginelli A, Napoli M, Fonio P, Briganti F. Neck neoplastic conditions in the emergency setting: role of multi detector computed tomography. *Seminars in Ultrasound CT MRI*. 2012;33(5):443–448
7. Jung HS, Jee WH, McCauley TR et al. Discrimination of metastatic from acute osteoporotic compression spinal fractures with MR imaging. *Radiographics*. 2003;23(1):179–187
8. Gokalp G, Mutlu FS, Yazici Z, Yildirim N. Evaluation of vertebral bone marrow fat content by chemical-shift MRI in osteoporosis. *Skeletal Radiol*. 2011;40:577–85.
9. Eito K, Waka S, Naoko N, Makoto A, Atsuko H. Vertebral neoplastic compression fractures: assessment by dual-phase chemical shift imaging. *J Magn Reson Imaging*. 2004;20:1020-1024.
10. Ogura A, Hayakawa K, Maeda F, et al. Differential diagnosis of vertebral compression fracture using in-phase/opposed-phase and short TI inversion recovery imaging. *Acta Radiol*. 2012;53:450–5.

11. Cicala F, Briganti, Casale L, Rossi C, Cagini L, Cesarano E, Brunese L, Giganti M. Atraumatic vertebral compression fractures: differential diagnosis between benign osteoporotic and malignant fractures by MRI. *Musculoskelet Surg.* 2013;97 (Suppl 2):S169–S179
12. Dalia Z, Zidan, Lobna A, Habib, Nevine A, Chalabi et al. Quantitative chemical-shift MR imaging cutoff value: Benign versus malignant vertebral compression – Initial experience. *The Egyptian Journal of Radiology and Nuclear Medicine.* 2014;45,779–786
13. Eryl WK, Oh ES, Outwater EK. The utility of in-phase/opposed-phase imaging in differentiating malignancy from acute benign compression fractures of the spine. *AJNR.* 2006;27:1183-1188.
14. Disler DG, McCauley TR, Ratner LM, et al. In-phase and out of- phase MR imaging of bone marrow: prediction of neoplasia based on the detection of coexistent fat and water. *AJR Am J Roentgenol.* 1997;169:1439–47.
15. Geith T, Schmid G. Comparison of Qualitative and Quantitative Evaluation of Diffusion- Weighted MRI and Chemical-Shift Imaging in the Differentiation of Benign and Malignant Vertebral Body Fractures. *AJR.* 2012;199:1083–1092.
16. Swartz PG, Roberts CC. Radiological reasoning: bone marrow changes on MRI. *AJR.* 2009, 193 [suppl]:S1–S4.

## Tables

**Table 1: Distribution of the patients according to the final diagnosis (No=20).**

Final diagnosed lesions	Number	%
Malignant causes	8	40.0
Breast cancer	1	5.0
Histiocytosis	2	10.0
Cancer Prostate	2	10.0
Metastases of unknown origin (Anaplastic Ca & lymphoma)	2	10.0
Non –malignant causes	3	15.0
Trauma	1	5.0
Osteoporosis	1	5.0
Kummel’s disease in a patient with HCC.		
Osteoporotic collapse in patient with cancer ovary		
Total	20	100.0

**Table 2: Associated radiological findings with vertebral collapse lesions.**

Associated radiological findings	Male	Female	Total
Epidural soft tissue component	3	2	5 (25%)
Spinal cord compression	1	1	2 (10%)
Degenerative disc affection	5	3	8 (40%)
Other distal fractures	0	1	1 (5%)
Other soft tissue lesions	1	1	2 (10%)
Other metastatic lesions	3	10	13 (65%)
Deformity	1	2	3 (15%)

**Table 3: SIR of the collapsed vertebrae.**

Case	Diagnosis	No of Vertebrae	SIR	Malignant or Nonmalignant
1	Breast cancer Metastasis	1	0.94	Malignant
2	Cancer prostate Metastasis	3	1.4	Malignant
3	MUO( anaplastic Ca)	1	1	Malignant
4	Breast cancer Metastasis	14	1.1	Malignant
5	Breast cancer Metastasis	4	0.92	Malignant
6	Cancer prostate Metastasis	1	1.38	Malignant
7	Breast cancer Metastasis	1	1	Malignant
8	Breast cancer Metastasis	1	1.45	Malignant
9	Breast cancer Metastasis	1	1.03	Malignant
10	Osteoporosis	1	0.58	Non malignant
11	Osteoporosis	1	0.48	Non malignant
12	Cancer ovary patient	5	0.6	Non malignant
13	Kummel's disease in HCC patient	1	1.1	Non malignant
14	Old trauma	1	0.37	Non malignant
15	Acute trauma	1	0.59	Non malignant
16	Osteoporosis	1	0.23	Non malignant
17	Breast cancer Metastasis	1	1.045	Malignant
18	Breast cancer Metastasis	5	1.06	Malignant
19	Histiocytosis	8	0.905	Malignant
20	MUO( lymphoma)	3	0.93	Malignant

MUO: metastasis of unknown origin.

**Table 4: DWI of the collapsed vertebrae.**

Case	Diagnosis	No of Vertebrae	Diffusion	ADC	Malignant or Nonmalignant
1	Breast cancer mets	1	Restricted	0.73	Malignant
2	Cancer prostate	3	Restricted	0.565	Malignant
3	MUO (Anaplastic)	1	Restricted	1	Malignant
4	Breast cancer mets	14	Restricted	0.769	Malignant
5	Cancer breast mets	4	Restricted	0.619	Malignant
6	Cancer prostate mets	1	Restricted	0.75	Malignant
7	Cancer breast mets	1	Restricted	0.68	Malignant
8	Cancer breast mets	1	Restricted	0.637	Malignant
9	Cancer breast mets	1	Restricted	0.98	Malignant
10	Osteoporosis	1	Not Restricted	1.45	Non malignant
11	Osteoporosis	1	Not Restricted	1.327	Non malignant
12	Cancer ovary patient	5	Not Restricted	1.08	Non malignant
13	Kummel's disease in HCC patient	1	Restricted	0.9	Non malignant
14	Old trauma	1	Not Restricted	1.29	Non malignant
15	Acute trauma	1	Not Restricted	1.38	Non malignant
16	Osteoporosis	1	Not Restricted	1.45	Non malignant
17	Cancer Breast mets	1	Restricted	0.769	Malignant
18	Cancer Breast mets	5	Restricted	0.78	Malignant
19	Histiocytosis	8	Not restricted	1.24	Malignant
20	MUO (lymphoma)	3	Restricted	1	Malignant

**Table 5: Scoring system of different imaging modalities in assessment of collapsed vertebrae.**

Case	Diagnosis	Conventional MRI	SIR	Diffusion	Score	Malignant or Nonmalignant
1	Breast cancer mets	Convex posterior border Hypo T1, Hyper T2	0.94	R	3	Malignant
2	Cancer prostate mets	Hypo T1, Heterogenous Hyper T2	1.4	R	2	Malignant
3	MUO( Anaplastic)	Convex posterior border Hypo T1, Hyper T2 Epidural mass	1	R	3	Malignant
4	Breast cancer mets	Epidural mass Iso T1, Hyper T2	1.1	R	3	Malignant
5	Cancer breast mets	Iso T1, Hyper T2 posterior neural arch involvement	0.92	R	3	Malignant
6	Cancer prostate mets	Hypo T1, Hypo T2 Epidural mass	1.38	R	3	Malignant
7	Cancer breast mets	Hypo T1, Hypo T2	1	R	2	Malignant
8	Cancer breast mets	Hypo T1, Hypo T2 Convex posterior border Epidural mass	1.45	R	3	Malignant
9	Cancer breast mets	Hypo T1, Hyper T2	1.03	R	2	Malignant
10	Osteoporosis	Hypo T1, Heterogenous Hyper T2	0.58	NR	0	Non malignant
11	Osteoporosis	Hypo T1, Hypo T2	0.48	NR	0	Non malignant
12	Cancer ovary patient	Iso T1, Hyper T2	0.6	NR	0	Non malignant
13	Kummel's disease	Hypo T1, Iso T2	1.1	R	2	Non malignant

14	Old trauma	Hypo T1, Hypo T2	0.37	NR	0	Non malignant
15	Acute trauma	Hypo T1, HyperT2	0.59	NR	0	Non malignant
16	Osteoporosis	Hypo T1, Iso T2	0.23	NR	0	Non malignant
17	Cancer Breast	Hypo T1, Iso T2	1.045	R	2	Malignant
18	Cancer Breast	Hypo T1, HyperT2,	1.06	NR	1	Malignant
19	Histiocytosis	Iso T1, Iso T2, Epidural mass	0.901	NR	1	Malignant
20	MUO (Lymphoma)	Hypo T1, Iso T2	0.93	R	2	Malignant

Mets: metastasis

**Table 6: Comparison between the signal intensities of the benign and malignant compression fracture in T1 and T2 WI.**

	T1			T2		
	Hypo	Hyper	ISO	hypo	Hyper	ISO
Malignant	10	0	3	3	7	3
Non malignant	6	0	1	2	3	2

**Table 7: Comparison between nonmalignant and malignant according to SIR.**

	Non-Malignant (n=7)	Malignant (n=13)	Control
SIR			
Min. – Max.	0.23 – 1.10	0.901 – 1.45	0.12 – 0.7
Mean ± SD.	0.56 ± 0.27	1.09 ± 0.20	0.51 ± 0.14
Median	0.58	1.03	0.55
Z (p)	2.855* (0.004*)		

Z: Z for Mann Whitney test

\*: Statistically significant at  $p \leq 0.05$

**Table 8: Sensitivity, specificity and accuracy for SIR.**



		Non malignant	Malignant	Sensitivity	Specificity	PPV	NPV	Accuracy
SIR	≤0.9	6	1	92.31	85.7	92.31	95.71	90.0
	>0.9	1	12					

**Table 9: Agreement for the imaging score system.**

	No.	%
Agree		
Malignant	12/13	92
Non malignant	6/7	85
Not agree		
Malignant	1/13	8
Non malignant	1/7	15

## Figures

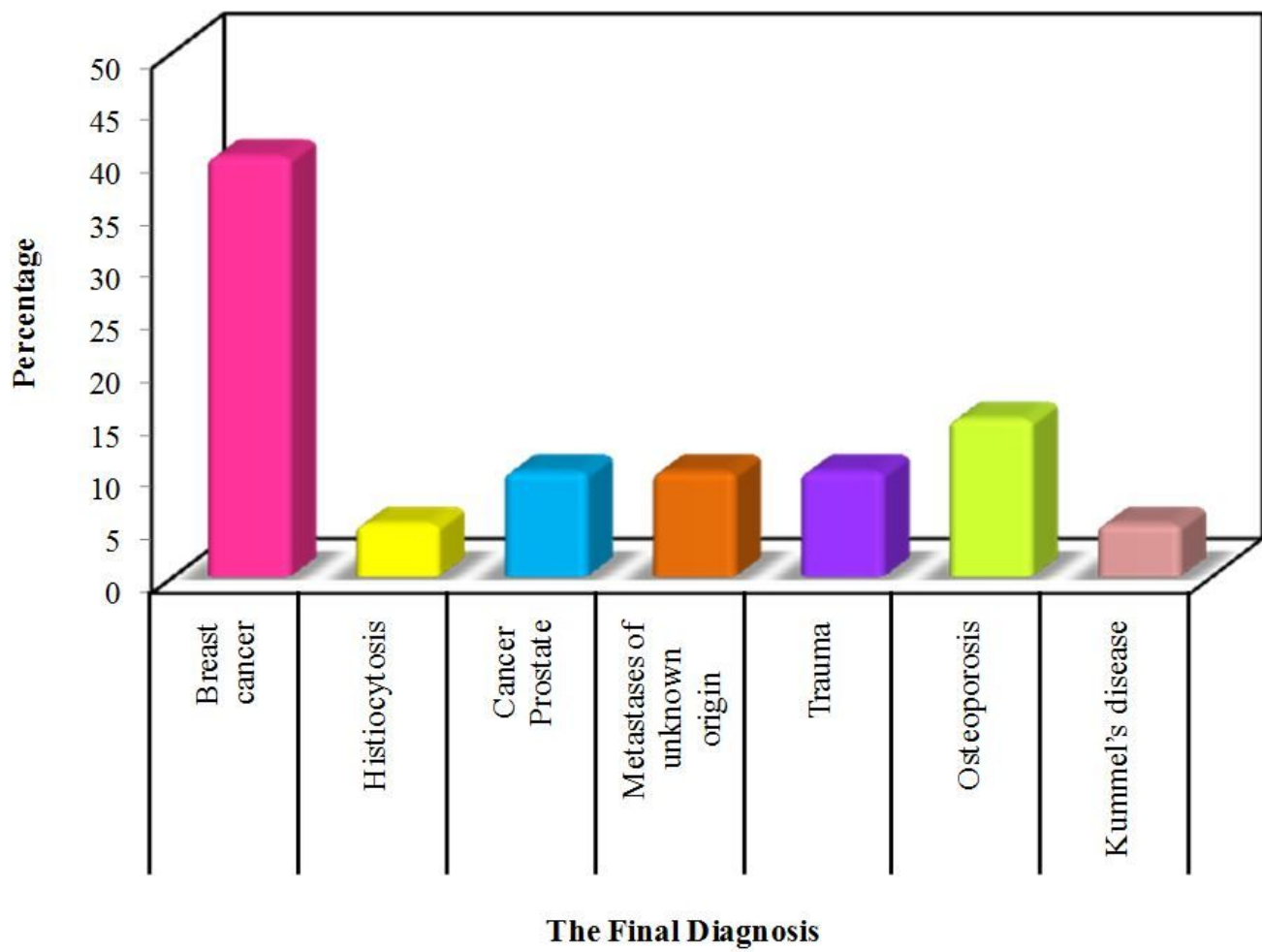


**Figure 1**

Distribution of the patients according to the final diagnosis

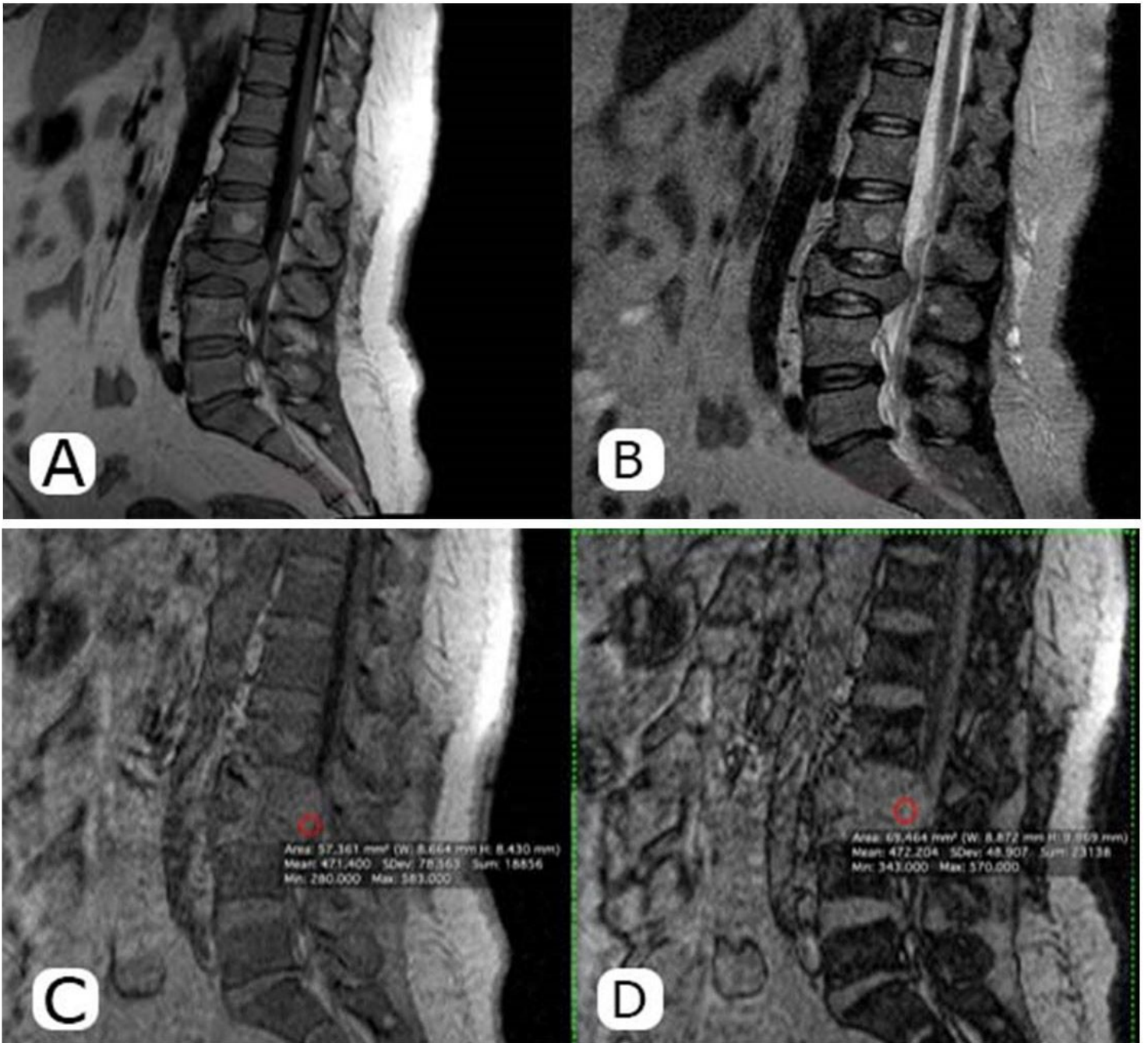


**Figure 2**

A 54 years old female patient, with history of cancer breast, complaining with low back pain as well as hepatic and osseous deposit. A) Sagittal T1, revealed markedly diminished height of LV3, with convex posterior border with T1 isointensity. Also noted LV2 vertebral body hemangioma. B) Sagittal T2WI, revealed iso to hyperintense signal. C) In phase sequence. D) Out of phase showing no definite signal drop, with SIR OP/IP > 0.9. Diffusion sequence revealed restricted diffusion, with ADC < 1.9 (not shown) Scoring system: 3 OPINION: Metastatic malignant vertebral compression fracture based on follow up and bone scan.

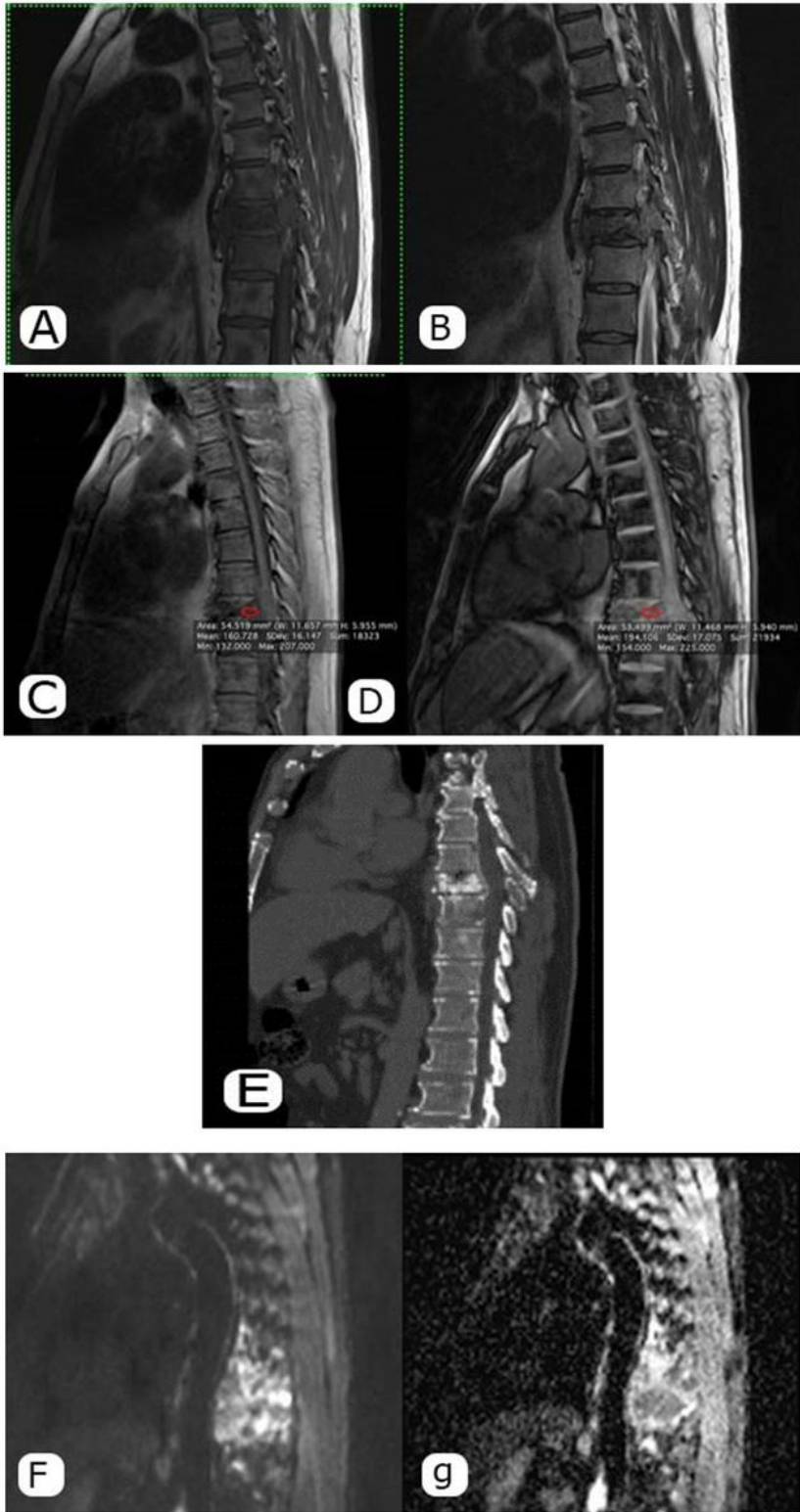


**Figure 3**

A 57 years old male patient with known history of cancer prostate, with sclerotic osseous metastasis on CT and positive serial bone scans. A) Sagittal T1, revealed diminished height of DV8, with diffuse T1 hypo intensity, associated with soft tissue pre and para vertebral component. B) Sagittal T2WI, revealed hypo intense signal of DV8. C) In phase sequence. D) Out of phase showing no definite signal drop, with SIR OP/IP > 0.9. E) Sagittal CT reconstruction, revealed diffusely sclerotic bony lesion, involving DV8. F,G)

Diffusion weighted image, showing definite restriction. ADC value  $<1$ , ( $0.68 \times 10^{-3}$ ) of the epidural component. Scoring system: 3 DIAGNOSIS: Metastatic vertebral collapse from cancer prostate on follow up and serial bone scans.

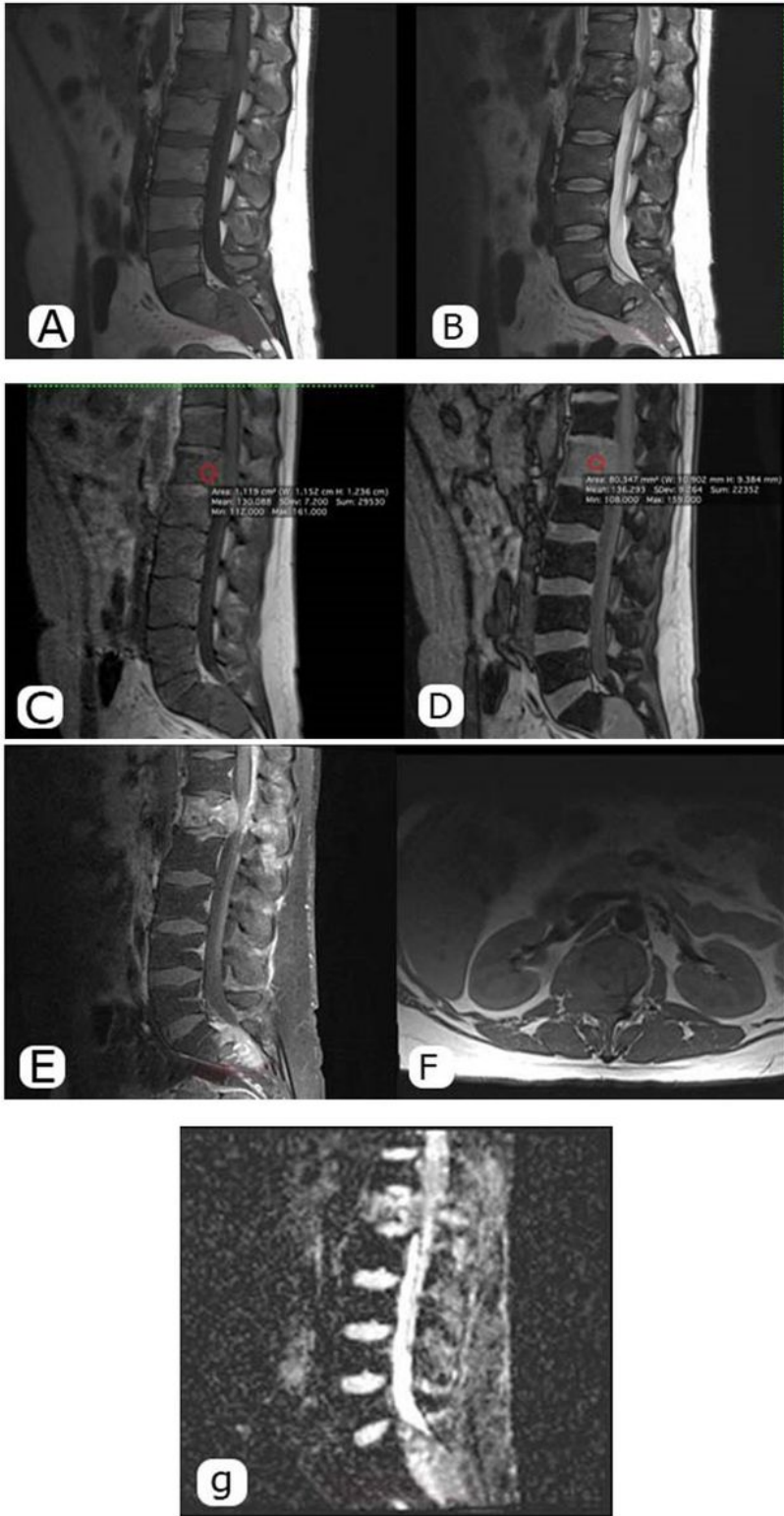
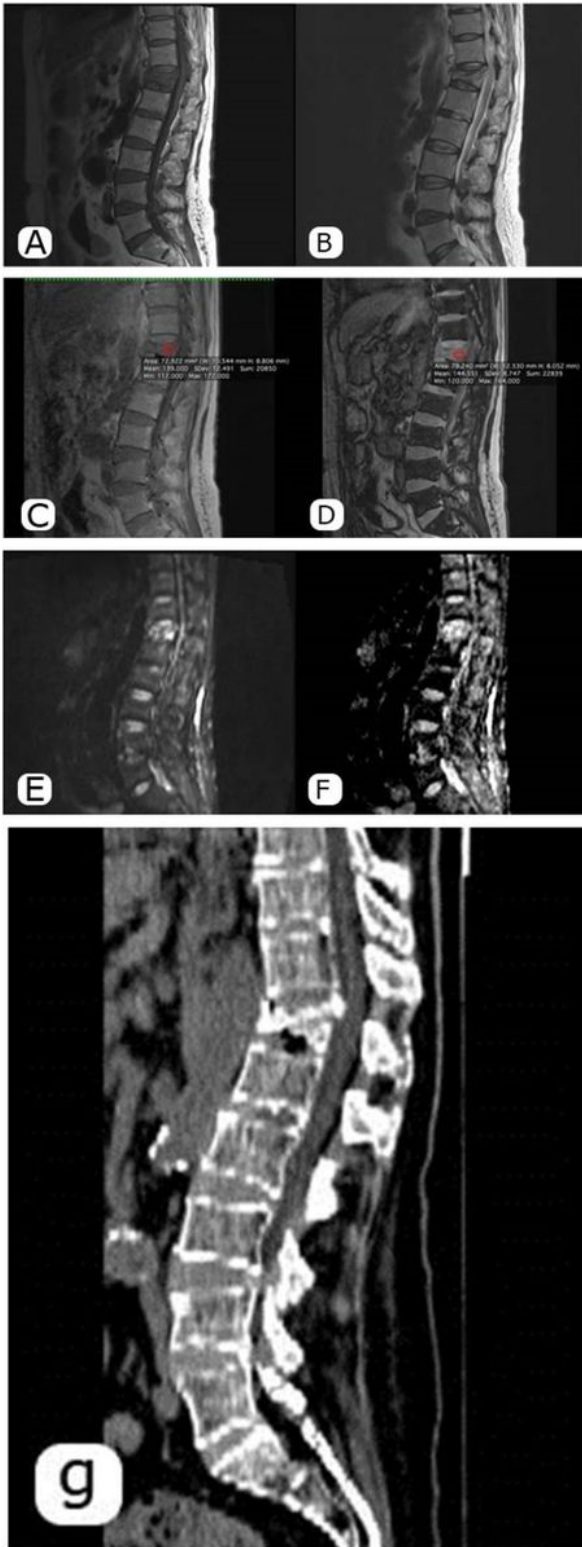


Figure 4

A 34 years old male patient, complaining of low back pain and sciatica, with no history of primary malignancy, showed accidental discovery of multiple osseous lesions, bone biopsy was done and

revealed metastatic deposits from primary anaplastic carcinoma. A) Sagittal T1, revealed markedly diminished height of LV1, with convex posterior border, related enhancing soft tissue epidural component opposite to LV1 & SV1, with diffuse T1 heterogeneous hypo intensity of the affected vertebra. B) Sagittal T2WI, revealed heterogeneous hypointense, with areas of hyper intensity. C) In phase sequence. D) Out of phase showing no definite signal drop, with SIR OP/IP > 0.9. Axial T1. E) Sagittal T1 post contrast fat saturation, revealed an enhancing epidural soft tissue component, encroaching on the spinal canal, more on the right side (best seen in axial T1), with another soft tissue enhancing component, seen opposite to SV1. F) T1 axial G) Diffusion weighted image ADC value < 1. Scoring system: 3 DIAGNOSIS: Metastatic vertebral collapse secondary to primary anaplastic carcinoma (Histopathologically proven).



**Figure 5**

A 67 years old male patient with history of primary hepato cellular carcinoma, complaining of low back pain, with serial follow up on CT, which showed a compressed vertebra. A) Sagittal T1, revealed anterior wedging of DV12, with heterogenous T1 hypointensity, with related intervertebral hypointense signals, and related to vacuum phenomenon. B) Sagittal T2WI, revealed heterogenous isointense signal. C) In phase sequence. D) Out of phase showing no definite signal drop, with SIR OP/IP > 0.9. E) Diffusion

weighted image, showing definite restriction. F) ADC value <1. G) Sagittal CT reconstruction revealed DV12 degenerative changes, in the form of diminished anterior height, focal cortical bony defect with intra as well as inter vertebral vacuum, serial follow up on CT, revealed stationary course of the affected vertebrae. No de novo lesions. Scoring System: 2 DIAGNOSIS: Serial follow up with stationary course, are more inclined to degenerative vertebral osteo necrosis (Kummel's disease).

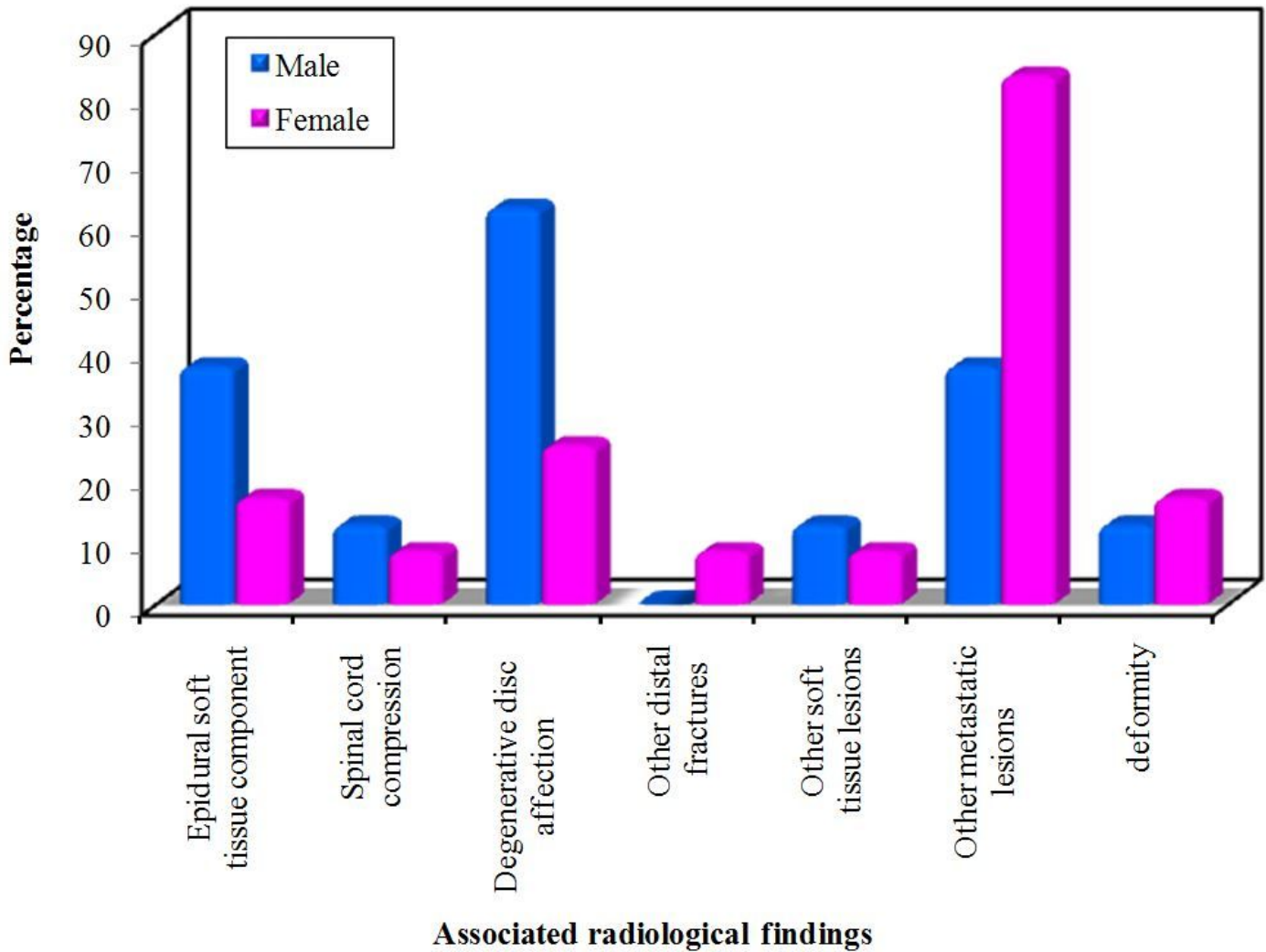


**Figure 6**

Associated radiological findings with vertebral collapse lesions.



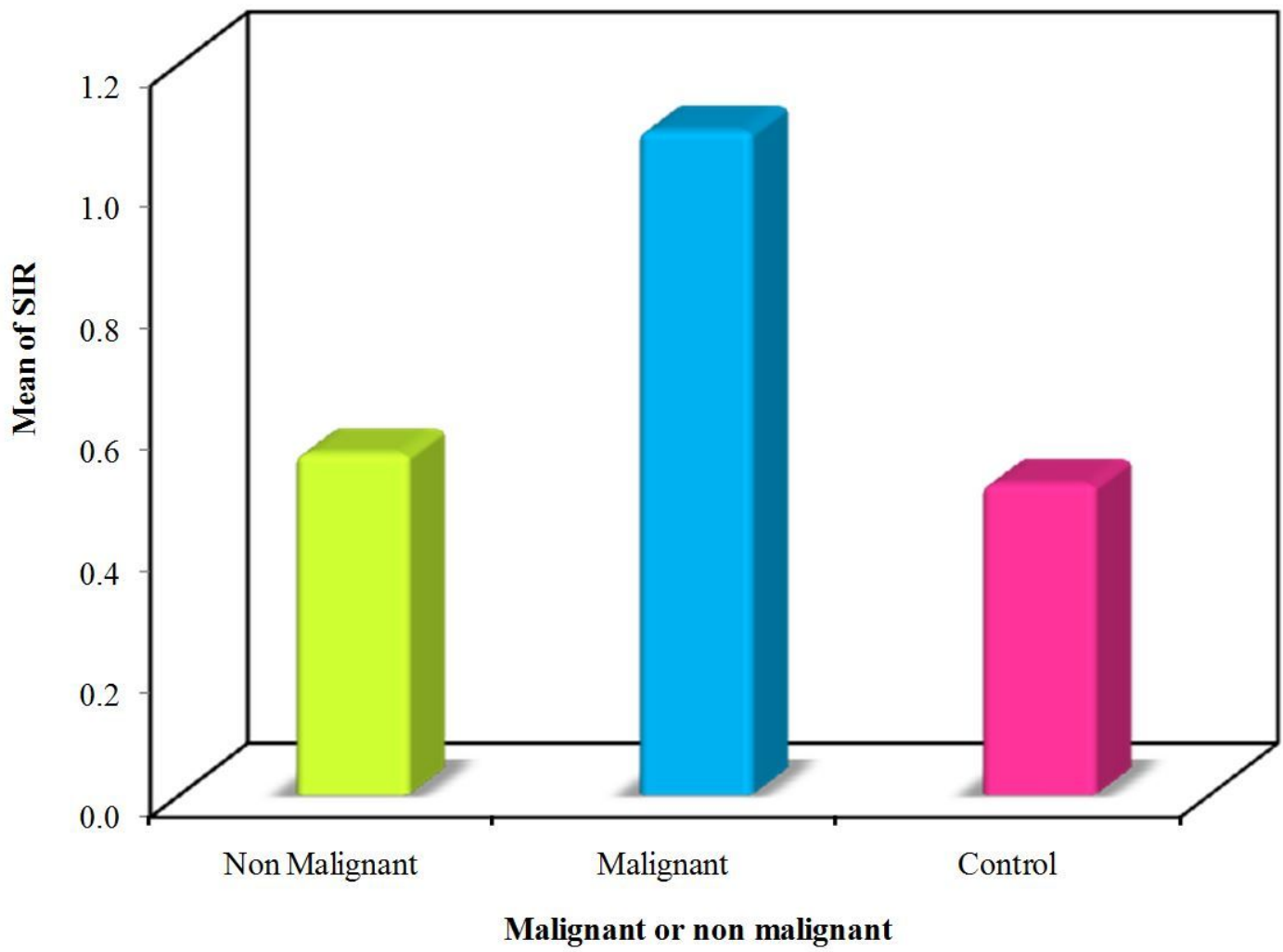


**Figure 7**

The signal intensity ratio (SIR): Relation between malignant and nonmalignant

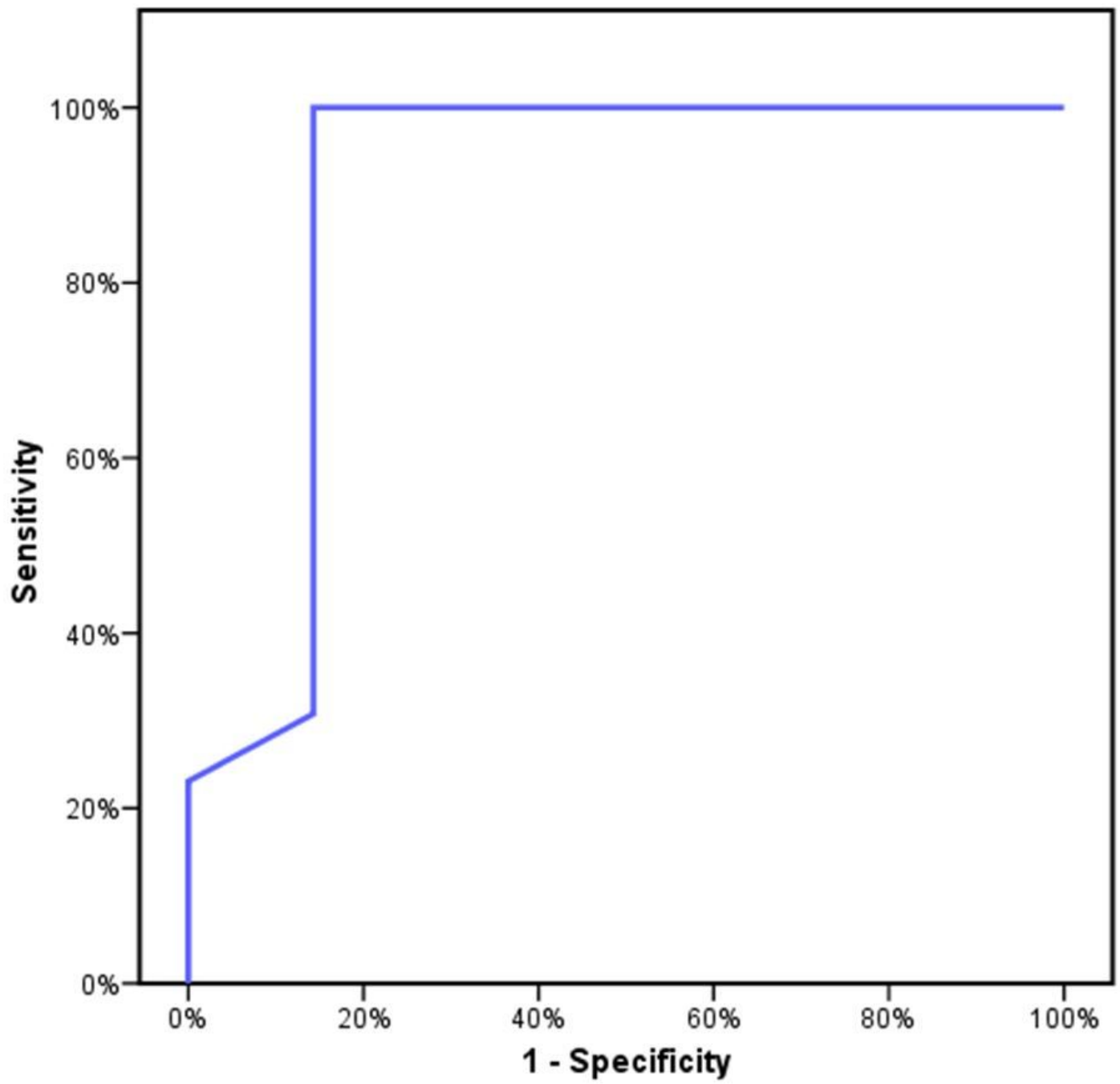


Figure 8

ROC curve for the signal intensity ratio (SIR)